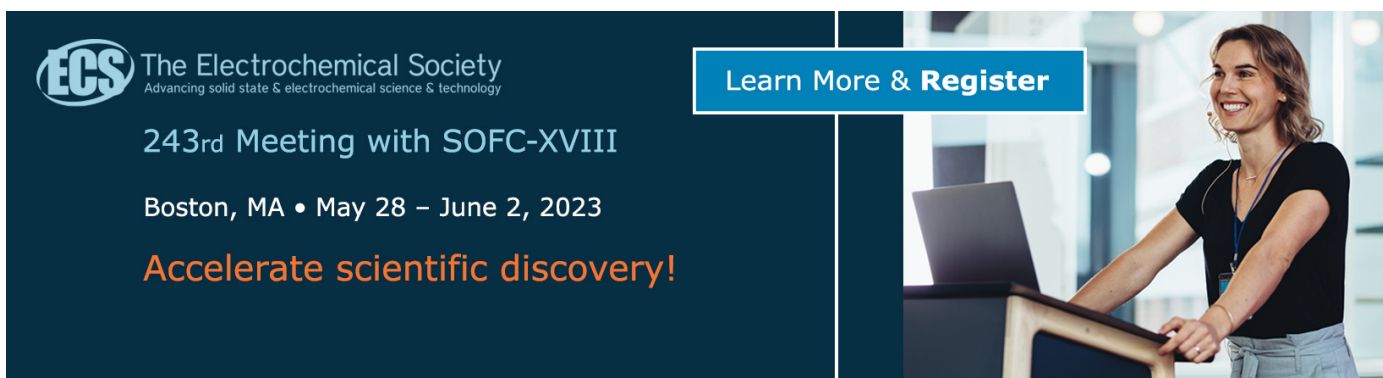


PAPER • OPEN ACCESS

Experimental Characterization of the Airflow within a Car Cabin

To cite this article: M. Bertone *et al* 2023 *J. Phys.: Conf. Ser.* **2509** 012024

View the [article online](#) for updates and enhancements.



The banner features a dark blue background on the left with white and orange text, and a photograph of a woman at a podium on the right. A blue button with white text is overlaid on the image.

 The Electrochemical Society
Advancing solid state & electrochemical science & technology

243rd Meeting with SOFC-XVIII

Boston, MA • May 28 – June 2, 2023

Accelerate scientific discovery!

Learn More & Register

Experimental Characterization of the Airflow within a Car Cabin

Authors: M. Bertone^{1,*}, A. Sciacchitano², F. Arpino¹, C. Canale¹, G. Cortellessa¹, G. Grossi¹, L. Moretti¹

¹ Department of Civil and Mechanical Engineering, University of Cassino and Southern Lazio, via G. Di Biasio 43, Cassino, Italy

² Faculty of Aerospace Engineering, Delft University of Technology, Kluyverweg 1, Delft, The Netherlands

* Corresponding author's e-mail address: michele.bertone@unicas.it

Abstract. The ventilation flow in a car cabin has been experimentally investigated. The study has been carried out in a car commercially available, by testing one ventilation mode (panel-vent mode) at one fan strength (level 3 of the 4 available) with fresh air intake (without any recirculation). The flow velocity at the exit of the vents has been measured using a 5-hole pressure probe. The flow velocity fields inside the car cabin have been measured by particle image velocimetry (PIV) in three longitudinal sections: (i) the car centre plane, including both the front and rear area; (ii) the driver's seat centre plane, only in the front area; (iii) the passenger's seat centre plane, only in the front area. At these longitudinal planes, the time-average flow velocity is presented and discussed. The experimental results provide new insights in the ventilation flow in a car cabin.

1. Introduction

The car cabin is an indoor micro-environment, where people spend a considerable amount of time [1, 2]; therefore, thermal comfort and indoor air quality play a key role and need to be considered to ensure the well-being of the occupants. To estimate and improve such parameters, accurate information about the car cabin environment is crucial, especially on the ventilation [3].

Previous studies on ventilation flow within the car cabin have used Computational Fluid Dynamics (CFD) simulations or experiments carried out with scaled or simplified models. Lee and Yoon [3] used a 1/10-scale car model to visualise the airflow inside the cabin and to measure the variation in temperature fields. Yang et al. [4] employed a car model made of acrylic material and an heating, ventilation and air-conditioning (HVAC) device to simulate ventilation conditions; the authors performed Particle Image Velocimetry (PIV) measurements to characterize the air flow inside the acrylic cabin and compared their results with those obtained by CFD simulations. Inside the cabins of actual cars, PIV measurements are often hindered by the limited access for the illumination and imaging systems. As a consequence, researchers had to perform geometrical modifications to the cars to guarantee the optical access. For instance, Lee et al. [5] replaced both the roof and the door passenger's seat part replaced with tempered glass to perform PIV in longitudinal planes. Similarly, Huera-Huarte et al. [6] removed the two doors of the co-pilot side and replaced them with two acrylic sheets to carry



out PIV measurements in longitudinal and horizontal planes. Ullrich et al. [7] performed PIV measurements in a car with the HVAC unit without the filter and compared the results with a CFD study. The flow within the car cabin is hard to study due to its dependence on several parameters, such as the position and shape of the vents, mode of ventilation, fan strength (air flow rate), geometry and size of the cabin [8, 9]. In all experimental studies reported in the literature, the car model used was scale-down or simplified, reducing or replacing interior vehicle elements. Therefore, the previous studies analyse the ventilation flow in the cabin in experimental conditions that are quite different from the operating conditions of a real vehicle. To overcome this limitation and to ensure a trustable reproduction of actual operating conditions, an experiment with a real car is needed.

In the present study, a real car was used to study the effect of ventilation on the flow field in the car cabin. The velocity fields of the ventilation flow inside the cabin were measured using the PIV measurement technique at three characteristic longitudinal planes; a 5-hole pressure probe was employed to measure the flow velocity at the outlet of the vents. The aim of this paper is to present a comprehensive benchmark for one ventilation mode (panel-vent mode) at a fixed fan speed of the car ventilation system useful for the validation of Computational Fluid Dynamics (CFD) numerical simulations. Measurements at all four fan speeds has been also investigated and will be presented in future papers. Validated numerical model can be used to investigate Indoor Air Quality (IAQ) and comfort of the occupants for the analyzed or any other car cabin.

2. Methodology

The experiments were carried out in a real car, a Peugeot 206; the measures of the car are 1430 mm (width) x 1430 mm (height) x 3835 mm (length). A schematic of the car with the main measures is shown in Figure 1.

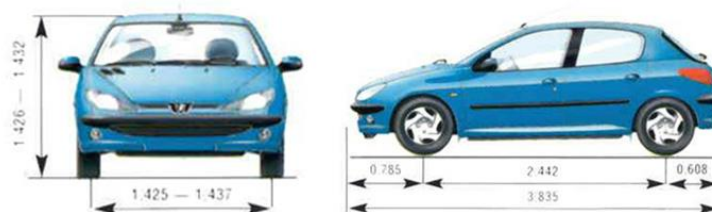


Figure 1 - View of the car with the main measures in metres.

The panel-vent mode was tested under one fan strength, at level 3 out of the 4 available for mass flow rate regulations and using fresh air intake (without any re-circulation). The panel-vent mode is such that each of the four inlet vents in the dashboard panel, indicated with numbers 3 and 4 in Figure 2, are open, while all the other vents are closed. The fans grille has been positioned with a neutral tilt and fixed with clips, according to previous studies by Adhikari et al. [10] and Piovano et al. [11], showing that an accurate fixing position of the grille is decisive for a repeatable examination of the air distribution in a car cabin.



Figure 2 – View of the cabin car with all the vents highlighted. In the current experiments, only the vents indicated with 3 and 4 were open, whereas all the others were kept closed.

No modifications have been made to the interior parts of the car cabin, including the seats, side doors, ceiling, and floor. Only the reflecting surfaces inside the cabin have been covered with non-reflecting material to avoid interferences in the processing of the collected data.

The flow velocity for each opening vent has been individually measured using a 5-hole pressure probe to allow investigation of the flow structures associated with each vent to give a proper definition of such boundary conditions. Despite the ventilation inducing a complex 3-dimensional flow in the car cabin, the planar PIV method has been used, since the lateral flow motion is quite weak in comparison to the vertical and longitudinal velocity components [12].

A preliminary study on the identification of the exit sections was performed; the ventilation system was seeded with water-glycol droplets of 1 μm median diameter produced by the SAFEX seeding generator. The flow patterns have been observed within the cabin, identifying by visual inspections the sections where the airflow exited. From this preliminary investigation, it was noticed that the air exited the cabin from several locations, being the vehicle not hermetic; however, a larger amount of air exited from the rear area of the passenger compartment, which is consistent with what reported in the study of Ullrich et al. [7].

2.1. Airflow at vents outlet, 5-hole pressure probe

A multi-hole pressure probe, the ProCap Compact 5-hole digital probe by Streamwise, has been used to obtain a 3D measurement of the airflow velocity exits of the vents. The 5-hole probe allows obtaining a 3D measurement of the flow velocity, determining the velocity, yaw angle, and pitch angle from measurements of the differential pressure [13] between pairs of holes located near the tip of the sensors [14]; a detailed description of the 5-hole probe is available in Paul et al. [15].

For each vent, a control volume has been defined and the measurements were carried out with an acquisition frequency of 60 Hz, with a sampling of 20 minutes for each vent. In post-processing, to show the velocity field, a surface parallel to the plane of the vents has been selected at a distance of approximately 1 cm from the latter.

2.2. PIV experimental setup

Planar PIV measurements at three longitudinal sections have been performed: (i) the car centre plane, including both the front and rear area (shown in Figure 3, detail a); (ii) the driver's seat centre plane, only at the front area (shown in Figure 3, detail b); (iii) the passenger's seat centre plane, only at the front area (shown in Figure 3, detail c). Each of these three different setups has required specific positioning of the cameras and laser head and specific system calibration.

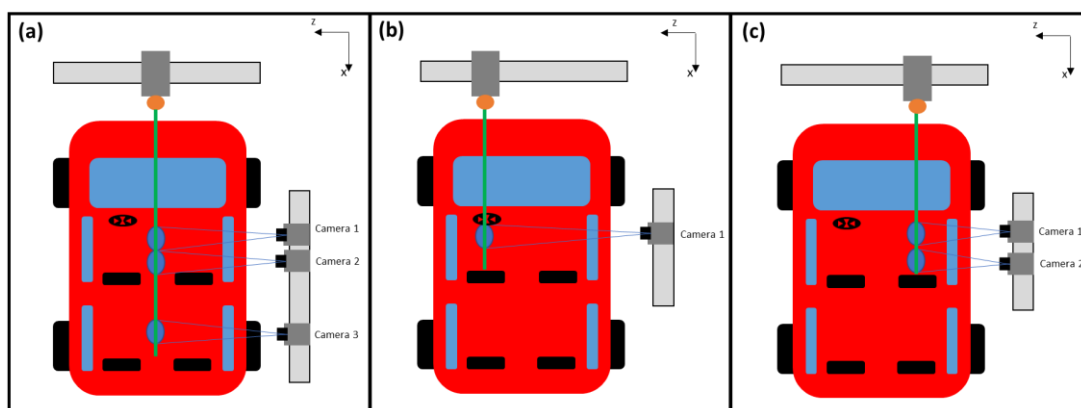


Figure 3 - PIV setup: (a) the car centre plane, including both the front and rear area; (b) the driver's seat centre plane (only the front area); (c) the passenger's seat centre plane (only the front area).

The experiment has been conducted in the backyard of the Aerodynamics Laboratories of the Delft University of Technology. To protect the equipment (seeding generator, laser, cameras and computer) in case of rain, and to confine the laser light, the car and the equipment have been placed inside a tent

of size 3 m (width) x 2.6 m (height) x 6 m (length). The temperature and humidity of the environment inside the tent have been checked during all the measurements, as well as the internal temperature of the cabin (summarized in Table 1). The seeding was generated using a SAFEX seeding generator, which produces water-glycol droplets of 1 μm median diameter. During the experiment, for all measurements performed, the seeding has been directly introduced inside the car cabin placing the SAFEX seeding generator inside. The particles were illuminated by a dual-cavity Evergreen Laser (Nd: YLF, pulse energy of 200 mJ at 15 Hz, wavelength of 532 nm) and images were recorded with three LaVision CMOS cameras (6.5 μm pixel size, 2560 \times 2160 pixels maximum resolution, 12 bit). Depending on the setup (see Figure 3), three, two or one cameras have been used. The cameras have been equipped with a Nikon object of 35 mm and 50 mm focal length and 4 or 5.6 as optical aperture, depending on the camera. The field of view and the optical magnification factor changed based on the setup and camera used. For setup (a) and setup (b), the cameras 1 and 2 were set in a way that the FOVs of each camera were overlapping between them, to obtain a larger image composed using the 2 images acquired by each camera (see section 3.2). In overlapping areas, arithmetic mean has been used to determine the velocity. Focal length, optical aperture, field of view and optical magnification factor are summarized in Table 1. The image acquisition has been conducted at a frequency of 15 Hz, except for the acquisition at setup (a) with camera 3, which is conducted at a frequency of 5 Hz. The time intervals between two consecutive particle images varied between 1 and 8 ms, depending on the camera used. Table 1 summarizes the main experimental parameters used in each configuration.

Table 1- summary of all parameters used during the acquisition

	Camera	f #	Lens objective (mm)	Field of view (mm)	Magnification factor	Frequency (Hz)	Δt (ms)	Temp out ($^{\circ}\text{C}$)	Humidity (%)	Temp in ($^{\circ}\text{C}$)
Setup a	1	5.6	35	653 x 545	0.025	15	1	30.2	28	43.6
	2	4	50	454 x 382	0.037	15	1	30.2	28	43.6
	3	4.6	35	472 x 397	0.035	5	2	28.4	25	37.8
Setup b	1	5.6	35	813 x 688	0.02	15	8	27.0	30	39.0
Setup c	1	5.6	35	524 x 437	0.032	15	5	29.1	33	39.5
	2	4	50	351 x 297	0.047	15	1.7	29.2	33	39.8

The data sets consist of 500 double-frame images for each experimental condition. The processing has been conducted via the LaVision Davis 8.6 software, using Gaussian interrogation windows of 128 \times 128 pixels with 75% overlap for the initial passes and 32 \times 32 pixels with 75% overlap for the final passes. The resulting instantaneous velocity fields have been ensemble-averaged to obtain the spatial distribution of the time-average velocity.

3. Results and discussions

The results from the experiments are presented in two sections; the first one discusses the results obtained from the 5-hole pressure probe for characterization of the airflow exits from the vents, whereas the second section discusses the PIV results in the longitudinal planes.

3.1. Airflow measurement at vents outlet, 5-hole pressure probe

Figure 4 shows the mean velocity fields of the outlet flow rate from the four vents opened in the panel-vent mode. The velocity fields show an asymmetry, as the velocity fields on the right (passenger's side) result in a higher magnitude than the velocity field on the left (driver's side). This is probably due to the design of the Peugeot 206 car, where the air intake duct is located on the right of the car hood. This influences the flow pattern inside the car cabin, as shown in section 3.2. Moreover, the shape of the mean velocity field from the vent at the left of the driver seat is quite different with respect to the others, which could be due to the presence of the steering wheel that has an influence on the velocity field.

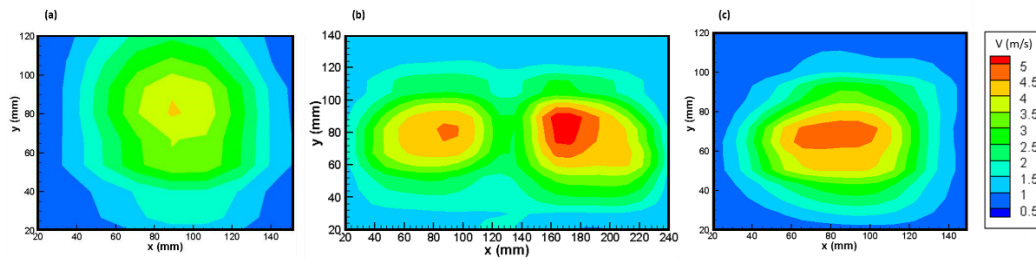


Figure 4 - mean velocity field in m/s of inlet flow rate from the vents active in panel-vent mode: (a) left vent, near the driver seat; (b) central vents; (c) right vent, near the passenger seat

3.2. Airflow measurement at longitudinal planes, PIV

Figure 5 shows the mean velocity fields at all measurement regions. The flow structure is complicated and large- and small-scale vortices coexist in the car cabin.

In Figure 5, detail a, the jet stream issued from the central dashboard vents is directly observed thanks to the measurement plane aligned at the centre of the two central panel vents. The jet stream is narrow and concentrated, probably due to the high fan strength (level 3 of the 4 available), the vents' shape and the tilt of the vents' grille. The flow issued impinges on the vehicle ceiling, leading to the formation of a large-scale clockwise vortex that characterizes both the front and rear area. From the rear area, part of the airflow is re-circulating through the vortex from the rear to the front area and part of the airflow goes to the parcel shelf, the section identified as the flow exit from the cabin. Despite the qualitative preliminary investigation has shown that the flow exits the passenger compartment in multiple locations, including the parcel shelf, the PIV measurement has confirmed that the flow of air is directed in that area, which can be considered the exit area. On average, the magnitude of the velocity vectors in the rear part is smaller than those in the front compartment. The region of the image that is affected by reflection due to the presence of the steering wheel, near the inlet section ($x = 0.15$ m, $y = 0.1$ m), has been masked.

In front of the driver's seat (Figure 5, detail b), two vortices rotating in opposite directions, one clockwise near the seat and one anti-clockwise near the windscreen, are located. Despite the fan strength imposed being very high (level 3 out of the 4 available), the magnitude of the vector in this area is small in comparison to the central plane.

In the passenger seat (Figure 5, detail c), the flow pattern is complicated and the magnitude of the velocity is larger compared with those of the driver's seat and smaller compared with those in the central plane. This may be caused by the different layout of the vehicle dashboard due to the different configurations required for the driver and passenger, such as the steering wheel at the driver's seat, which could cause an asymmetry in the flow. The asymmetry could be also due to the difference in the magnitude of the velocity flow in the outlet vents active in the panel-vent mode, greater on the vents on the right than on the vents on the left (see paragraph 3.1).

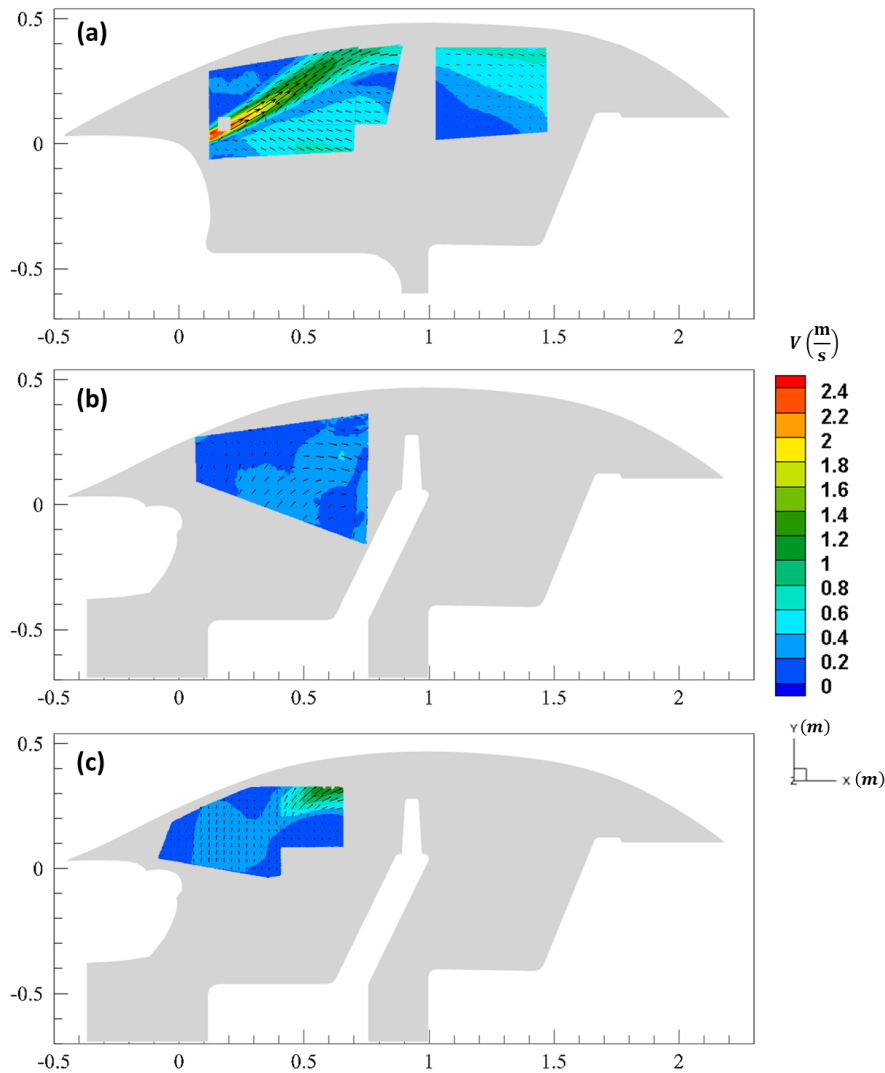


Figure 5 - mean velocity fields in the x-y plane inside the car cabin: (a) the car centre plane, including both the front and rear area; (b) the driver's seat centre plane (only the front area); (c) the passenger's seat centre plane (only the front area).

Figure 6 shows (a) mean velocity and (b) measurement uncertainty at a 95% confidence level carried out at the car centre longitudinal plane (front area). The airflow velocity reaches a maximum velocity of 2.4 m/s in the jet stream near the outlet of the fans and decreases considerably from a point around 0.4 m. The uncertainty of the jet stream is around 0.055 m/s in the core zone, and reduces to 0.04 m/s in the tail area.

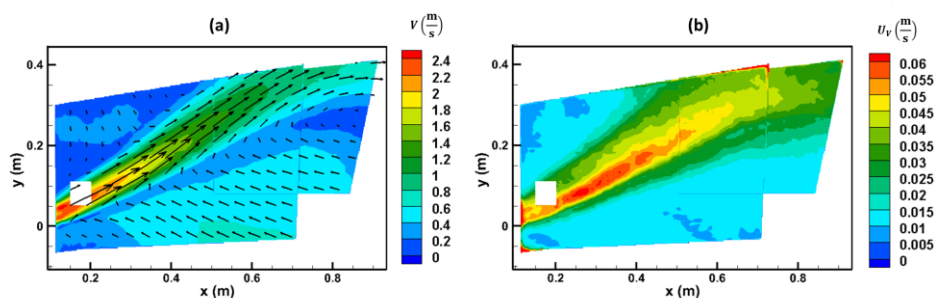


Figure 6 - (a) mean velocity fields and (b) uncertainty (both in meters per second) at the car centre plane (front area)

Figure 7 shows measurements of the (a) mean velocity and (b) measurement uncertainty at a 95% confidence level carried out in a longitudinal plane that goes through the middle of the car in the rear area. The magnitude of velocity vectors is around 0.4 m/s and the uncertainty is around 0.03 m/s.

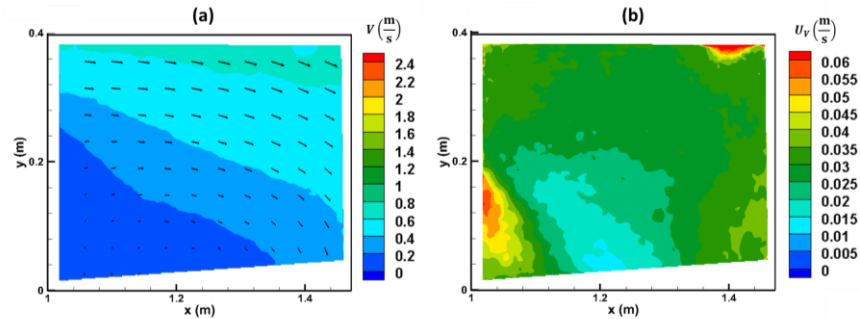


Figure 7 - (a) mean velocity fields and (b) uncertainty (both in meters per second) at the car centre plane (rear area)

Figure 8 shows (a) mean velocity and (b) measurement uncertainty at a 95% confidence level carried out at the longitudinal plane that goes through the centre of the driver seat. The maximum velocity is 0.5 m/s and the magnitude of the velocity vectors is smaller than those in the front compartment.

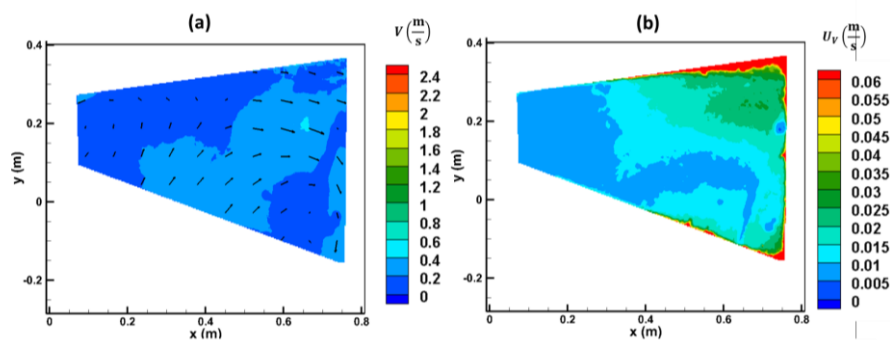


Figure 8 - (a) mean velocity fields and (b) uncertainty (both in meters per second) at the central section of the driver's seat

Figure 9 shows measurements carried out in the longitudinal plane that goes through the passenger's seat. The maximum velocity is 1 m/s.

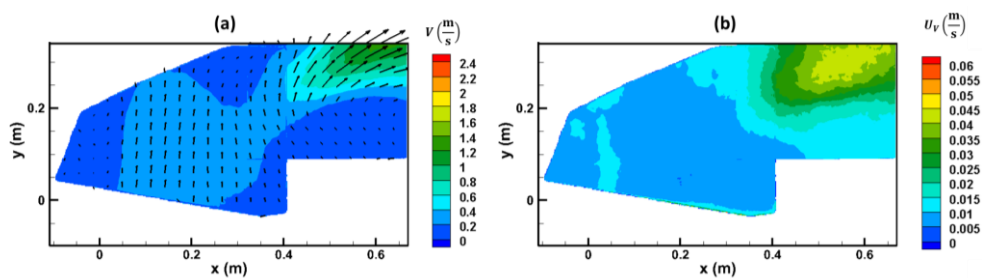


Figure 9 - (a) mean velocity fields and (b) uncertainty (both in meters per second) at the central section of the passenger seat

4. Conclusions

The ventilation flow in a car cabin has been experimentally investigated with the aim to propose a comprehensive benchmark for Computational Fluid Dynamics (CFD) numerical simulations validation. The study has been carried out in a commercial car cabin without any internal or external modification, by testing one ventilation mode (panel-vent mode) at one fan strength (level 3 of the 4 available) with fresh air intake (without any re-circulation). Obtained data represent preliminary results of an experimental campaign in which the velocity airflow field at all four fan speeds has been investigated. The results refer to the outgoing velocity field of vents active in panel-vent mode, measured using a 5-hole pressure probe and to three characteristic longitudinal planes, measured using the PIV technique.

The velocity field on the outgoing velocity field from the vents has shown an asymmetry between vents on the left and right sides, a difference which also occurs in the velocity field measured with the PIV in the driver's and passenger's plans. On the longitudinal centre plane, the jet stream outgoing from the vents is narrow and concentrated and the flow issued impinges the vehicle ceiling, leading to the formation of a large-scale clockwise vortex that characterizes both the front and rear area. The experimental results allow a better understanding of the ventilation flow in a car cabin and allows the construction of a benchmark case for the validation of CFD numerical simulations. Validated numerical model represents a useful tool for the design and optimization of the ventilation system to improve Indoor Air Quality (IAQ) and comfort of the occupants in any car cabin. Measurements at all four fan speeds has been also investigated and will be presented in future papers.

References

- [1] G. Buonanno, G. Giovinco, L. Morawska, and L. Stabile, 'Tracheobronchial and alveolar dose of submicrometer particles for different population age groups in Italy', *Atmos. Environ.*, vol. 45, no. 34, pp. 6216–6224, Nov. 2011, doi: 10.1016/j.atmosenv.2011.07.066.
- [2] European Communities, 'How Europeans spend their time', Luxemburg: European Communities, 2004.
- [3] S.-J. Lee and J.-H. Yoon, 'Temperature field measurement of heated ventilation flow in a vehicle interior', *Int. J. Veh. Des.*, vol. Vol. 19, no. No. 2, p. pp 228-243, 1998.
- [4] J. H. Yang, S. Kato, and H. Nagano, 'Measurement of airflow of air-conditioning in a car with PIV', *J. Vis.*, vol. 12, no. 2, pp. 119–130, Jun. 2009, doi: 10.1007/BF03181954.
- [5] J. P. Lee, H. L. Kim, and S. J. Lee, 'Large-scale PIV measurements of ventilation flow inside the passenger compartment of a real car', *J. Vis.*, vol. 14, no. 4, pp. 321–329, Dec. 2011, doi: 10.1007/s12650-011-0095-9.
- [6] F. J. Huera-Huarte, X. Cort, E. Aramburu, X. Vizcaino, and L. Casto, 'DPIV Measurements of the HVAC Aerodynamics Inside a Passenger Car', *SAE Tech. Pap.*, pp. 2014-36–0214, Sep. 2014, doi: <https://doi.org/10.4271/2014-36-0214>.
- [7] S. Ullrich, R. Buder, N. Boughanmi, C. Friebe, and C. Wagner, 'Numerical Study of the Airflow Distribution in a Passenger Car Cabin Validated with PIV', in *New Results in Numerical and Experimental Fluid Mechanics XII*, vol. 142, A. Dillmann, G. Heller, E. Krämer, C. Wagner, C. Tropea, and S. Jakirlić, Eds. Cham: Springer International Publishing, 2020, pp. 457–467. doi: 10.1007/978-3-030-25253-3_44.
- [8] F. Arpino *et al.*, 'Risk of SARS-CoV-2 in a car cabin assessed through 3D CFD simulations', *Indoor Air*, vol. 32, no. 3, Mar. 2022, doi: 10.1111/ina.13012.
- [9] F. Arpino, G. Cortellessa, G. Grossi, and H. Nagano, 'A Eulerian-Lagrangian approach for the non-isothermal and transient CFD analysis of the aerosol airborne dispersion in a car cabin', *Build. Environ.*, vol. 209, p. 108648, Feb. 2022, doi: 10.1016/j.buildenv.2021.108648.
- [10] V. P. Adhikari, A. Nassar, and Q. H. Nagpurwala, 'Numerical Studies on the Effect of Cooling Vent Setting and Solar Radiation on Air Flow and Temperature Distribution in a Passenger Car', *Numer. Stud. Eff. Cool.*, pp. 2009-28–0048, Dec. 2009, doi: 10.4271/2009-28-0048.
- [11] A. Piovano, L. Loreface, N. Paola, L. Miretti, and E. Ribaldone, 'Automated CFD multi-objective optimization for a passenger vehicle panel duct', 2014.
- [12] J.-H. Yoon and S.-J. Lee, 'Velocity field measurements of ventilation flow in a vehicle interior', *Int. J. Veh. Des.*, vol. 31, no. 1, p. 96, 2003, doi: 10.1504/IJVD.2003.002050.
- [13] R. Robinson, D. Butterfield, D. Curtis, and T. Thompson, 'Problems with Pitots. Issues with flow measurement in stacks', *International Conference on Emission Monitoring*, Milan (Italy), 2004.
- [14] Denis William Bryer and R. C. Pankhurst, 'Pressure-probe Methods for Determining Wind Speed and Flow Direction', *Aeronaut. J.*, vol. 75, p. 660, 1971, doi: 10.1017/S0001924000046315.
- [15] A. Paul, R. Upadhyay, and A. Jain, 'A novel calibration algorithm for five-hole pressure probe', *Int. J. Eng. Sci. Technol.*, vol. 3, no. 2, Jul. 2011, doi: 10.4314/ijest.v3i2.68136.